



King Saud University
Arabian Journal of Chemistry

www.ksu.edu.sa
www.sciencedirect.com



REVIEW

Essential oil of *Salvia aucheri mesatlantica* as a green inhibitor for the corrosion of steel in 0.5 M H₂SO₄

M. Znini^a, L. Majidi^{a,*}, A. Bouyanzer^c, J. Paolini^b, J.-M. Desjobert^b,
J. Costa^b, B. Hammouti^c

^a Laboratoire des Substances Naturelles & Synthèse et Dynamique Moléculaire, Faculté des Sciences et Techniques, Errachidia, Morocco

^b Université de Corse, UMR CNRS 6134, Laboratoire de Chimie des Produits Naturels, Faculté des Sciences et Techniques, Corse, France

^c Laboratoire de Chimie Appliquée et Environnement, Faculté des Sciences, Oujda, Morocco

Received 12 May 2010; accepted 17 September 2010

Available online 23 September 2010

KEYWORDS

Corrosion;
Inhibition;
Steel;
Essential oil;
Salvia aucheri mesatlantica;
Adsorption

Abstract Essential oil of aerial parts of *Salvia aucheri* Boiss. var. *mesatlantica* was obtained by hydrodistillation and analyzed by GC and GC/MS. The oil was predominated by camphor (49.59%). The inhibitory effect of this essential oil was estimated on the corrosion of steel in 0.5 M H₂SO₄ using electrochemical polarization and weight loss measurements. The corrosion rate of steel is decreased in the presence of natural oil. The inhibition efficiency was found to increase with oil content to attain 86.12% at 2 g/L. Polarization curves revealed that the oil of *S. aucheri mesatlantica* acts as mixed type inhibitor with a strong predominance of anodic character. The temperature effect on the corrosion behavior of steel in 0.5 M H₂SO₄ without and with the inhibitor at 2 g/L was studied in the temperature range from 303 to 343 K, the associated activation energy have been determined. The adsorption of oil on the steel surface was found to obey Langmuir's adsorption isotherm.

© 2010 King Saud University. Production and hosting by Elsevier B.V. All rights reserved.

* Corresponding author. Tel.: +212 0661422903; fax: +212 0535574485.

E-mail address: .



Contents

1. Introduction	468
2. Experimental	468
2.1. Plant material	468
2.2. Hydrodistillation apparatus and procedure	468
2.3. GC analysis	468
2.4. Gas chromatography–mass spectrometry	469
2.5. Components identification	469
2.6. Weight loss, polarization and EIS measurements	469
3. Results and discussion	469
3.1. <i>Salvia aucheri</i> var. <i>mesatlantica</i> oil analysis	469
3.2. Corrosion tests	469
3.2.1. Weight loss tests	469
3.2.2. Polarization measurements	470
3.2.3. Electrochemical impedance spectroscopy (EIS)	471
3.3. Effect of temperature	472
3.4. Adsorption isotherm	473
4. Conclusions	473
References	473

1. Introduction

Acid solutions are generally used for the removal of undesirable scale and rust in several industrial processes. Hydrochloric and sulfuric acids are widely used in the pickling processes of metals (Chauhan and Gunasekaran, 2007). The use of inhibitors is one of the best methods of protecting metals against corrosion (Eddy and Ebenso, 2008; Eddy and Odoemelam, 2008). Most corrosion inhibitors are organic compounds having hetero-atoms in their aromatic or long carbon chain (Eddy and Ebenso, 2008; Eddy and Odoemelam, 2008; Al-Sehaibani, 2000). The efficiency of these compounds as corrosion inhibitors can be attributed to the number of mobile electron pair present, the orbital character of free electrons and electron density around the hetero-atoms (Azhar et al., 2001). However, there is increasing concern about the toxicity of most corrosion inhibitors. The toxic effect does not only affect living organisms but also poison the environment (Eddy and Ebenso, 2008; Eddy and Odoemelam, 2008).

Due to the toxicity of some corrosion inhibitors, there has been increasing search for green corrosion inhibitors (Al-Sehaibani, 2000). Inhibitors in this class are those that are environmentally friendly and are obtained from natural products such as plant extracts (Avwiri and Igho, 2001). Recently, several studies have been carried out on the inhibition of corrosion of metals by plant extract (El-Ashry et al., 2006; Sethuran and Raja, 2006), essential oils (Bouyanzer et al., 2007; Faska et al., 2007) or purified compounds (Chaieb et al., 2005; Faska et al., 2008). We previously reported that Pennyroyal oil (Bouyanzer et al., 2006a), Eucalyptus oil (Bouyanzer et al., 2006b), Jojoba oil (Chetouani et al., 2004), Rosemary oil (Bendahou et al., 2006; Chaieb et al., 2004; El-Ouariachi et al., 2010), Artemisia oil (Ouachikh et al., 2009; Benabdellah et al., 2006; Bouyanzer and Hammouti, 2004), Lavender oil (Zerga et al., 2009), Menthol derivatives (Faska et al., 2007), Eugenol and Acetyleneugenol (Chaieb et al., 2005), Pulegone (Faska et al., 2008) and Limonene (Chaieb et al., 2009) have been found to be very efficient corrosion

inhibitors for steel in acid media. In this paper, our choice is focused to essential oil of *Salvia aucheri* Boiss. var. *mesatlantica*. We have noted that *S. aucheri* var. *mesatlantica*, a species of the family Lamiaceae (Ozcan, 2005), is a hermaphrodite and a subshrub endemic to the region of Errachidia (south-eastern Morocco), it is known locally as the vernacular name “Tagoltante”. Local people used the leaves and stems in decoction to treat stomach, digestive disorders and rheumatism.

The aim of this paper is to extract and to test *S. aucheri* var. *mesatlantica* oil (SAMO) as corrosion inhibitor for steel in 0.5 M H₂SO₄ solution. The study is conducted by weight loss and electrochemical polarization methods. Discussion is based on the analysis of oil chemical composition.

2. Experimental

2.1. Plant material

The aerial part of *S. aucheri* var. *mesatlantica* was harvested in May 2007 in the wild in the mountain Assoul located at the south-east of Errachidia (Morocco). A voucher specimen was deposited in the Herbarium of Faculty of Sciences and Techniques, Errachidia, Morocco. The dried plant material is stored in the laboratory at room temperature (298 K) and in the shade before the extraction.

2.2. Hydrodistillation apparatus and procedure

The extraction of essential oil of the aerial part of *S. aucheri* was conducted by hydrodistillation using a Clevenger type apparatus (Clevenger, 1928), and the essential oil yield was 1.2%. The essential oil obtained was dried under anhydrous sodium sulfate and stored at 277 K in the dark before analysis.

2.3. GC analysis

GC analyses were performed using a Perkin-Elmer Autosystem GC apparatus (Walton, MA, USA) equipped with a single

injector and two flame ionization detectors (FID). The apparatus was used for simultaneous sampling to two fused-silica capillary columns (60 m × 0.22 mm, film thickness 0.25 μm) with different stationary phases: Rtx-1 (polydimethylsiloxane) and Rtx-Wax (polyethylene glycol). Temperature program: 333–503 K at 275 K/min and then held isothermal 503 K (30 min). Carrier gas: helium (1 mL min⁻¹). Injector and detector temperatures were held at 553 K. Split injection was conducted with a ratio split of 1:80. Injected volume: 0.1 μL.

2.4. Gas chromatography–mass spectrometry

The oils obtained were investigated using a Perkin-Elmer TurboMass Quadrupole Detector, directly coupled to a Perkin-Elmer Autosystem XL equipped with two fused-silica capillary columns (60 m × 0.22 mm, film thickness 0.25 μm), Rtx-1 (polydimethylsiloxane) and Rtx-Wax (polyethylene glycol). Other GC conditions were the same as described above. Ion source temperature: 423 K; energy ionization: 70 eV; electron ionization mass spectra were acquired with a mass range of 35–350 Da. Oil injected volume: 0.1 μL.

2.5. Components identification

Identification of the components was based (i) on the comparison of their GC retention indices (RI) on non-polar and polar columns, determined relative to the retention time of a series of n-alkanes with linear interpolation, with those of authentic compounds or literature data (König et al., 2001) and (ii) on computer matching with commercial mass spectral libraries (Adams, 2001; König et al., 2001) and comparison of spectra with those of our personal library. Relative amounts of individual components were calculated on the basis of their GC peak areas on the two capillary Rtx-1 and Rtx-Wax columns, without FID response factor correction.

2.6. Weight loss, polarization and EIS measurements

The aggressive solution (0.5 M H₂SO₄) was prepared by dilution of Analytical Grade 98% H₂SO₄ with double-distilled water. Prior to all measurements, the steel samples (0.09% P; 0.38% Si; 0.01% Al; 0.05% Mn; 0.21% C; 0.05% S and the remainder iron) were polished with emery paper up to 1200 grade, washed thoroughly with double-distilled water, degreased with AR grade ethanol, acetone and dried at room temperature.

Weight loss measurements were carried out in a double walled glass cell equipped with a thermostat-cooling condenser. The solution volume was 100 ml. The steel specimens used had a rectangular form (2 cm × 2 cm × 0.05 cm). The immersion time for the weight loss was 6 h at 298 K. After the corrosion test, the specimens of steel were carefully washed in double-distilled water, dried and then weighed. The rinse removed loose segments of the film of the corroded samples. Duplicate experiments were performed in each case and the mean value of the weight loss is reported. Weight loss allowed us to calculate the mean corrosion rate as expressed in mg cm⁻² h⁻¹.

Electrochemical measurements were carried out in a conventional three-electrode electrolysis cylindrical Pyrex glass cell. The working electrode (WE) in the form of disc cut from steel has a geometric area of 1 cm² and is embedded in polytet-

rafluoroethylene (PTFE). A saturated calomel electrode (SCE) and a disc platinum electrode were used, respectively, as reference and auxiliary electrodes. The temperature was thermostatically controlled at 298 ± 1 K. The WE was abraded with silicon carbide paper (grade P1200), degreased with AR grade ethanol and acetone, and rinsed with double-distilled water before use.

Running on an IBM compatible personal computer, the 352 Soft Corr™ III Software communicates with EG&G Instruments potentiostat–galvanostat model 263A at a scan rate of 0.5 mV/s. Before recording the cathodic polarization curves, the steel electrode is polarized at –800 mV for 10 min. For anodic curves, the potential of the electrode is swept from its corrosion potential after 30 min at free corrosion potential, to more positive values. The test solution is deaerated with pure nitrogen. Gas bubbling is maintained through the experiments.

The electrochemical impedance spectroscopy (EIS) measurements were carried out with the electrochemical system which included a digital potentiostat model Volta lab PGZ 100 computer at E_{corr} after immersion in solution without bubbling, the circular surface of steel exposing of 1 cm² to the solution was used as working electrode. After the determination of steady-state current at a given potential, sine wave voltage (10 mV) peak to peak, at frequencies between 100 kHz and 10 mHz was superimposed on the rest potential. Computer programs automatically controlled the measurements performed at rest potentials after 30 min of exposure. The impedance diagrams are given in the Nyquist representation. Values of R_t and C_{dl} were obtained from Nyquist plots.

3. Results and discussion

3.1. *Salvia aucheri* var. *mesatlantica* oil analysis

The analysis of *S. aucheri* var. *mesatlantica* essential oil (SAMO) allowed the identification of 38 components, which accounted for 95.20% in the total of oil. Their retention indices (RIs) and their relative percentages are reported in Table 1.

All these compounds were performed by comparing their EI-mass spectra and their RIs with those of our own library. *S. aucheri* var. *mesatlantica* essential oil was characterized by high content of monoterpenes (83.7%) while sesquiterpenes accounted only for 11.7%; it was dominated by oxygenated monoterpenes (67.9%) with camphor appearing as the major component with 49.8% followed by other components with relatively small amounts: 1,8-cineole (9.5%), viridiflorol (8.8%) and camphene (7.8%). The literature showed that no study has been done on the essential oil from *S. aucheri* var. *mesatlantica*. However, the camphor was found as the main constituent of essential oils of two variety of Turkey namely as *S. aucheri* Benth var. *canescens* (23.41%) (Ipek et al., 2008). *S. aucheri* Benth var. *aucheri* (21.1%) (Kürkcüoğlu et al., 2002) and a variety of Morocco called *S. aucheri* Benth subsp. *blancoana* (44.1%) (Holemen et al., 1984).

3.2. Corrosion tests

3.2.1. Weight loss tests

The corrosion rate (W_{corr}) of steel in 0.5 M H₂SO₄ solution at various contents of SAMO tested was determined after 6 h of

immersion period at 298 K. Values of corrosion rates and inhibition efficiencies are given Table 2. In the case of the weight loss method, the inhibition efficiency ($E_w\%$) was determined by the following relation:

$$E_w\% = \frac{W_{\text{corr}} - W_{\text{corr(inh)}}}{W_{\text{corr}}} \times 100 \quad (1)$$

where W_{corr} and $W_{\text{corr(inh)}}$ are the corrosion rates of steel in the absence and presence of the oil, respectively.

Table 1 Chemical composition of *S. aucheri* var. *mesatlantica* essential oil (SAMO).

No.	Components	RI l	RI a	RI p	%
1	Tricyclene	927	921	995	0.3
2	α -Pinene	936	930	1007	2.9
3	Camphene	950	943	1046	7.8
4	β -Pinene	978	967	1088	1.2
5	Myrcene	987	976	1132	0.2
6	p-Cymene	1015	1007	1229	1.5
7	1,8-Cineole	1024	1016	1183	9.5
8	Limonene	1025		1167	1.9
9	Camphenilone	–	1051	1407	0.2
10	Linalool	1086	1078	1498	0.2
11	α -Campholenal	1105	1096	1436	0.1
12	Camphor	1123	1119	1467	49.8
13	<i>trans</i> -Pinocarveol	1126		1599	1.0
14	<i>cis</i> -Verbenol	1132	1122	1626	0.4
15	Pinocarvone	1137	1132	1511	0.4
16	Borneol	1150	1143	1646	1.7
17	p-Cymen-8-ol	1169	1154	1789	0.5
18	Terpinen-4-ol	1164	1155	1551	0.4
19	Myrtenal	1172	1163	1570	0.5
20	α -Terpineol	1176	1166	1643	0.4
21	Myrtenol	1178	1174	1734	0.3
22	<i>trans</i> -Carveol	1200	1192	1777	0.3
23	Carvone	1214	1210	1673	0.2
24	Bornyl acetate	1270	1265	1529	1.0
25	Carvacrol	1278	1275	2135	0.5
26	α -Terpinyl acetate	1335	1329	1643	0.4
27	Geranyl acetate	1362	1358	1706	0.1
28	γ -Cadinene	1507	1506	1706	0.3
29	<i>trans</i> -Calamenene	1517	1509	1777	0.1
30	Caryophyllene oxide	1578	1569	1919	0.3
31	Globulol	1589	1575	1994	0.2
32	Viridiflorol	1592	1584	2021	8.8
33	Epoxyde d'Humulene II	1602	1594	1973	0.3
34	Caryophylla-4(14),8(15)-dien-5 α -ol	–	1621	2220	0.3
35	τ -Cadinol	1633	1627	2102	0.5
36	β -Eudesmol	1641	1636	2157	0.3
37	α -Cadinol	1643	1640	2161	0.3
38	Cadalene	1659	1657	2140	0.3
	Total identified				95.40
	Monoterpene hydrocarbons				15.80
	Oxygenated monoterpenes				67.90
	Hydrocarbonate sesquiterpenes				11.00
	Oxygenated sesquiterpenes				0.70

Order of elution is given on apolar column (Rtx-1).
 RI l = retention indices on the apolar column of literature.
 RI a = retention indices on the apolar column (Rtx-1).
 RI p = retention indices on the polar column (Rtx-Wax).
 % = relative percentages of components are given on the apolar column except for components with identical RI a (percentages are given on the polar column).

Table 2 Gravimetric results of steel corrosion in 0.5 M H₂SO₄ (6 h immersion) without and with various concentrations of SAMO at 298 K.

Inhibitors	Concentration	W (mg/h cm ²)	E_w (%)
H ₂ SO ₄	0.5 M	1.79	–
<i>Salvia aucheri mesatlantica</i> oil	0.25 g/L	0.389	78.25
	0.5 g/L	0.372	79.18
	1 g/L	0.319	82.13
	1.5 g/L	0.270	84.89
	2 g/L	0.248	86.12

The analysis of these results (Table 2) shows clearly that the corrosion rate decreases (W (mg/h cm²)) while the inhibition efficiency ($E_w\%$) increases with increasing inhibitor concentration reaching a maximum value of 86.12% at a concentration of 2 g/L. This behavior can be attributed to the increase of the surface covered θ ($E_w\%/100$), and that due to the adsorption of natural compounds on the surface of the metal, as the inhibitor concentration increases. We can conclude that SMAO is a good corrosion inhibitor for steel in 0.5 M H₂SO₄ solution.

3.2.2. Polarization measurements

The characteristics of current–potential curves resulting from cathodic and anodic polarization of steel in 0.5 M H₂SO₄ with various concentrations of SAMO have been evaluated. Fig. 1 shows the potentiodynamic polarization curves containing various concentrations of Sage oil at 298 K.

The corrosion parameters including corrosion current densities (I_{corr}), corrosion potential (E_{corr}), cathodic Tafel slope (β_c), anodic slope (β_a) and inhibition efficiency ($E_1\%$) are listed in Table 3. In the case of polarization method the relation determines the inhibition efficiency ($E_1\%$):

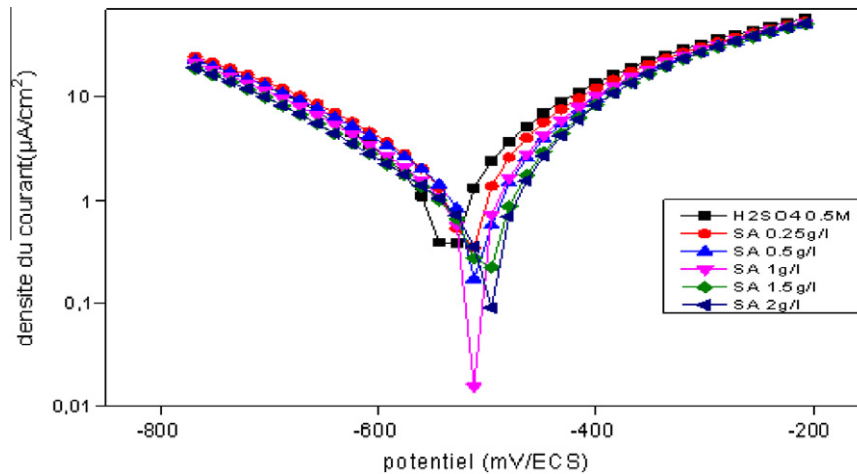
$$E_1\% = \frac{I_{\text{corr}} - I_{\text{corr(inh)}}}{I_{\text{corr}}} \times 100 \quad (2)$$

where I_{corr} and $I_{\text{corr(inh)}}$ are the corrosion current density values without and with the inhibitor, respectively, determined by extrapolation of cathodic Tafel lines to the corrosion potential.

From electrochemical polarization measurements, it is clear from the results that the addition of inhibitor causes a decrease of the current density. The values I_{corr} of steel in the inhibited solution are smaller than those for the inhibitor free solution (Table 3). This decrease can be explained by the inhibitory action of this inhibitor. The parallel cathodic Tafel plots obtained in Fig. 1 indicate that the hydrogen evolution is activation-controlled and the slight change of both β_c and β_a indicates that the reduction mechanism is not affected by the presence of inhibitor. In the domain anodic (Fig. 1), the polarization curves of steel have shown that the addition of the SAMO decreases the current density and moves the corrosion potential to positive values acting mainly on the dissolution reaction of metal. The inhibition efficiency ($E_1\%$) increases with inhibitor concentration reaching 85.45% at 2 g/L. However, at potentials higher than –240 mV/s, the presence of SMAO shows no effect on the anodic curves. This feature of the current is associated with the development of localized corrosion. These results suggest that the inhibitory action depends on the potential of SAMO and a desorption process appears at

Table 3 Polarization parameters and $E_1\%$ for steel corrosion in 0.5 M H_2SO_4 without and with various concentrations of SAMO at 298 K.

Inhibitors	Concentration	$-E_{corr}$ (mV/SCE)	I_{corr} (mA/cm ²)	β_a (mV/dec)	$-\beta_c$ (mV/dec)	$E_1\%$
H_2SO_4	0.5 M	572.7	2.6657	194.1	226.6	–
<i>Salvia oil</i>	0.25 g/L	557	0.6436	190.4	234.6	75.85
	0.5 g/L	549	0.4921	174.4	220.8	81.53
	1 g/L	557	0.4720	163	204.9	82.29
	1.5 g/L	554	0.4491	148.7	188.3	83.15
	2 g/L	553	0.3876	142.7	180	85.45

**Figure 1** Polarization curves of steel in 0.5 M H_2SO_4 without and with various concentrations of SAMO at 298 K.

high potential (Bentiss et al., 2002). These results suggest that this compound acts as a good corrosion inhibitor mixed character with a strong predominance of anodic character.

3.2.3. Electrochemical impedance spectroscopy (EIS)

The corrosion behavior of steel in 0.5 M H_2SO_4 solution with and without SAMO is also investigated by the electrochemical

impedance spectroscopy (EIS) at 298 K after 30 min of immersion. The charge-transfer resistance (R_t) values are calculated from the difference in impedance at lower and higher frequencies, as suggested by Tsuru et al. (1978). The double-layer capacitance (C_{dl}) and the frequency at which the imaginary component of the impedance is maximal ($-Z_{max}$) are found as represented in the following equation:

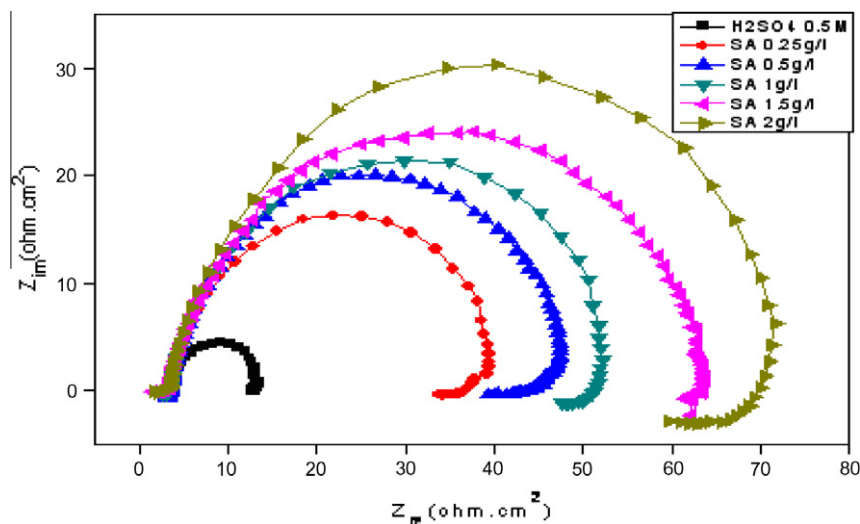
**Figure 2** Nyquist plots of steel in 0.5 M H_2SO_4 without and with various concentrations of SAMO at 298 K.

Table 4 Electrochemical impedance parameters and $E_{Rt}\%$ for steel corrosion in 0.5 M H_2SO_4 without and with various concentrations of SAMO at 298 K.

Inhibitors	Concentration	$-E_{corr}$ (mV/SCE)	$R_t(\Omega\text{ cm}^2)$	F_{max} (Hz)	C_{dl} ($\mu\text{F}/\text{cm}^2$)	$E_{Rt}\%$
H_2SO_4	0.5 M	572	10.88	316.46	3096	–
<i>Salvia oil</i>	0.25 g/L	557	34.65	100	287.84	68.60
	0.5 g/L	549	42.61	89.286	186.74	74.46
	1 g/L	557	48.68	79.365	154.94	77.64
	1.5 g/L	554	60.84	63.291	111.25	82.11
	2 g/L	553	68.72	40	76.42	84.16

$$C_{dl} = \frac{1}{2\pi f_{max} R_t} \quad (3)$$

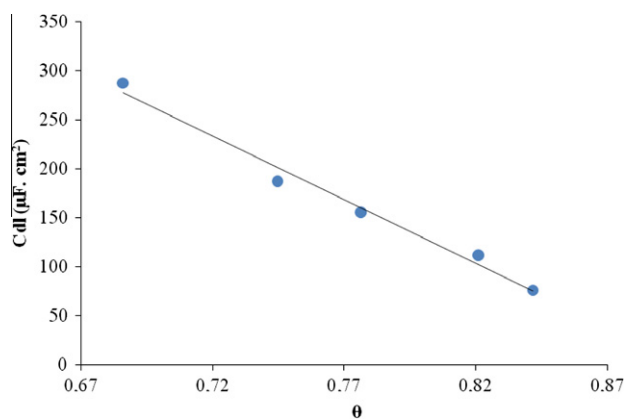
where f_{max} is the frequency at which the imaginary component of the impedance (Z_{im}) is maximum and R_t is the diameter of the loop.

Impedance diagrams are obtained for frequency range 100 KHz–10 mHz at the open circuit potential for steel in 0.5 M H_2SO_4 in the presence and absence of SMAO. Nyquist plots for steel in 0.5 M H_2SO_4 at various concentrations of SAMO is presented in Fig. 2. Table 4 gives values of charge-transfer resistance, R_t double-layer capacitance, C_{dl} , and f_{max} derived from Nyquist plots and inhibition efficiency, the inhibition efficiency got from the charge-transfer resistance is calculated by the following relation:

$$E_{Rt}\% = \frac{R'_t - R_t}{R'_t} \times 100 \quad (4)$$

R_t and R'_t are the charge-transfer resistance values without and with inhibitor, respectively.

Generally, Fig. 2 showed that the impedance spectra exhibit one single depressed semicircle, and the diameters of semicircle increases with the inhibitor concentration. The single semicircle can be attributed to the charge transfer that takes place at electrode/solution interface, and the transfer process controls the corrosion reaction of steel and the presence of inhibitor does not change the mechanism of dissolution of steel (Larabi et al., 2004). It is also clear that these impedance diagrams consists of one large capacitive loop and they are not perfect semicircles and this difference has been attributed to frequency dispersion Mansfeld et al., 1981, 1982 and the heterogeneity of the metal surface (Juttner, 1990; Pajkosay, 1994).

**Figure 3** The double-layer capacitance as function of the surface coverage.

From the electrochemical polarization data (Table 4), it is clear that the R_t values increase with inhibitor concentration and consequently the inhibition efficiency increases to 84.16% at 2 g/L. In fact, the presence of SAMO is accompanied by the increase of the value of R_t in acidic solution confirming a charge-transfer process mainly controlling the corrosion of steel. Values of double-layer capacitance are also brought down to the maximum extent in the presence of inhibitor and the decrease in the values of C_{dl} follows the order similar to that obtained for I_{corr} in this study. The decrease in C_{dl} is due to the adsorption of the inhibitor on the metal surface leading to the formation of film or complex from acidic solution (Bentiss et al., 1999).

We also note the increase of the value of R_t with the inhibitor concentration leading to an increase in the corrosion inhibition efficiency. A good agreement is observed between weight loss and electrochemical results.

A quick examination of the electrochemical and EIS parameters indicates that the values of the corrosion potential and cathodic Tafel slopes vary slightly in the presence of SAMO concentration. These results suggest that the action of molecules of natural oil act by pure geometric blocking of the electrode surface. The $E\%$ should coincide with θ (Cao, 1996). Also the linear decrease of C_{dl} with the surface coverage means that the capacitance contribution from the inhibitor-covered surface is solely due to the flat-adsorbed molecules at low surface coverage (Martinez and Metikos-Hukovic, 2003) (Fig. 3).

3.3. Effect of temperature

The effect of temperature on the corrosion behavior of steel in 0.5 M H_2SO_4 containing inhibitor at a concentration 2 g/L is studied in the temperature range 303–343 K using weight loss measurements at 2 h. The data of corrosion rates and corresponding efficiency collected are presented in Table 5.

Examination of Table 5 revealed that the corrosion rate increases both in the uninhibited and in the inhibited acid

Table 5 Gravimetric results of steel corrosion in 0.5 M H_2SO_4 (2 h immersion) without and with 2 g/L SAMO at different temperatures.

T (K)	W_{corr} ($\text{mg}/\text{cm}^2\text{ h}$)	$W_{corr(inh)}$ ($\text{mg}/\text{cm}^2\text{ h}$)	$E\%$
303	1.764	0.528	70.06
313	4.211	1.207	71.32
323	7.125	1.905	73.26
333	14	3.661	73.85
343	21.78	5.634	74.13

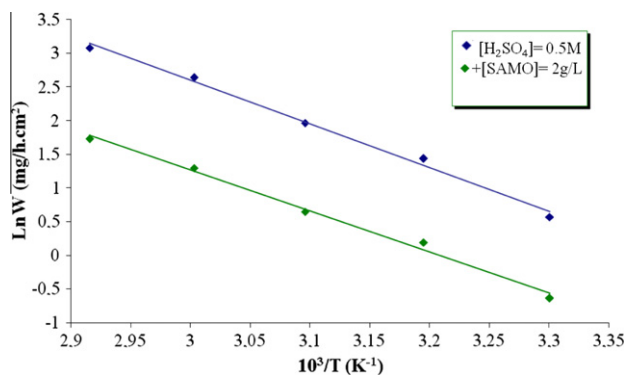


Figure 4 Arrhenius plots for the corrosion rate of steel in 0.5 M H_2SO_4 without and with SAMO at different temperatures.

solution with the rise of temperature. The presence of inhibitor leads to decrease of the corrosion rate. $E\%$ depends upon the temperature and increases with temperature. The increase in $E\%$ indicates that the inhibitory effect of SMAO is reinforced at elevated temperature.

In acidic solution, the corrosion rate is related to temperature by Arrhenius equation:

$$W_{\text{corr}} = k \exp(-E_a/RT) \text{ and } W'_{\text{corr}} = k' \exp(-E'_a/RT) \quad (5)$$

where, W'_{corr} and W_{corr} are the corrosion rates of steel with and without inhibitor, respectively. E'_a and E_a are the apparent activation energies in the presence and absence of inhibitor, respectively.

The apparent activation energy was determined from the slopes of $\ln W_{\text{corr}}$ vs $1/T$ graph depicted in Fig. 4.

The calculated values of activation energies from the slopes are 54 and 50.65 kJ/mol for free acid and with the addition of SAMO, respectively. We remark that the activation energy change slightly in the presence of inhibitor. Furthermore, the increase of $E\%$ is explained by Ammar and El Khorafi (1973) as chemisorption of inhibitor molecules on the steel surface. The lower value of E_a of the corrosion process in an inhibitor's presence when compared to that in its absence is attributed to its chemisorption (Popova et al., 2004).

3.4. Adsorption isotherm

Adsorption isotherms are very important to understand the mechanism of inhibition corrosion reactions. The most

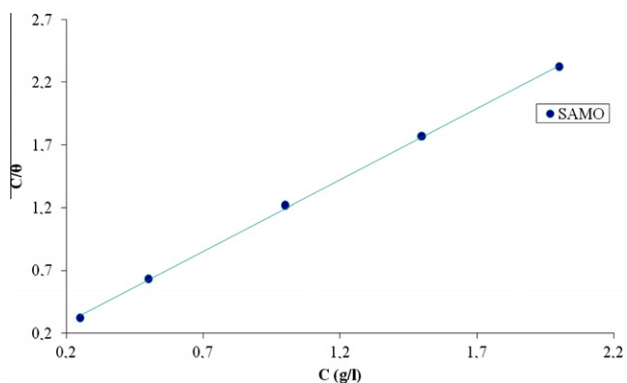


Figure 5 Langmuir adsorption isotherm of SAMO on steel surface from 0.5 M H_2SO_4 .

frequently used isotherms are Langmuir (Langmuir, 1947), Frumkin (Frumkin, 1925) and Temkin (de Boer, 1968). The Langmuir isotherm (C/θ vs C) assumes that there is no interaction between adsorbed molecules on the surface. The Frumkin adsorption isotherm (θ vs C) assumes that there is some interaction between the adsorbates, and the Temkin adsorption isotherm (θ vs $\lg C$) represents the effect of multiple layer coverage (Masel, 1996).

The dependence of the fraction of the surface covered θ obtained by the ratio $E\%/100$ as function of SAMO concentration (C) was graphically fitted for various adsorption isotherms.

Fig. 5 shows the dependence of θ as function of the logarithm of SAMO concentration. The curve obtained clearly shows that the data fit well with Langmuir adsorption isotherm was found to be the best description of the adsorption behavior of the studied inhibitor, which obeys:

$$\frac{C_{\text{inh}}}{\theta} = \frac{1}{b} + C_{\text{inh}} \quad (6)$$

C_{inh} is the inhibitor concentration; θ is the fraction of the surface covered, b is the adsorption coefficient.

The literature shows that the adsorption of heterocyclic compounds occurs with the aromatic rings mostly perpendicular with respect of the metal surface at low concentration, but at elevated inhibitor concentration the molecules are reoriented to the parallel mod (Bockris and Young, 1999). Besides, the adsorption phenomenon may be made by camphor as the principal constituent of the essential oil of *S. aucheri mesatlantica*. But as the natural oil contains so many components, the inhibitory action may be due to synergistic intermolecular of the active molecules of this oil.

4. Conclusions

From the overall experimental results the following conclusions can be deduced:

1. Chemical analysis shows that camphor can be the major component of *S. aucheri mesatlantica* oil.
2. *Salvia aucheri mesatlantica* oil mainly acts as good inhibitor for the corrosion of steel in 0.5 M H_2SO_4 .
3. Inhibition efficiency increases with both the concentration of inhibitor and the temperature.
4. The natural oil acts on steel surface as anodic inhibitor.
5. Inhibition efficiency on steel may occur by action of camphor.

References

- Adams, R.P., 2001. Identification of Essential Oil Components by Gas Chromatography/Quadrupole Mass Spectroscopy. Allured Publishing, Carol Stream.
- Al-Schaibani, A., 2000. Materialwiss. Werkstofftech. 31, 1060.
- Ammar, I.A., El Khorafi, F.M., 1973. Werkst. Korros. 24, 702.
- Avwiri, G.O., Igho, F.O., 2001. Mater. Lett. 57, 3705.
- Azhar, M.E., Mernari, M., Traisnel, M., Bentiss, F., Lagrenee, M., 2001. Corros. Sci. 43, 22.
- Benabdellah, M., Benkaddour, M., Hammouti, B., Bendahou, M., Aouiti, A., 2006. Appl. Surf. Sci. 252, 6212.

- Bendahou, M., Benabdellah, M., Hammouti, B., 2006. *Pigm. Resin Technol.* 35, 95.
- Bentiss, F., Lagrenée, M., Traisnel, M., Hornez, J.C., 1999. *Corros. Sci.* 41, 789.
- Bentiss, F., Traisnel, M., Chaïbi, N., Mernari, B., Vezin, H., Lagrenée, M., 2002. *Corros. Sci.* 44, 2271.
- Bockris, J.O.M., Young, B., 1999. *J. Electrochem. Soc.* 138, 2237.
- Bouyanzer, A., Hammouti, B., 2004. *Pigm. Resin Technol.* 33, 287.
- Bouyanzer, A., Hammouti, B., Majidi, L., 2006a. *Mater. Lett.* 60, 2840.
- Bouyanzer, A., Majidi, L., Hammouti, B., 2006b. *Bull. Electrochem.* 22, 321.
- Bouyanzer, A., Majidi, L., Hammouti, B., 2007. *Phys. Chem. News* 37, 70.
- Cao, C., 1996. *Corros. Sci.* 38, 2073.
- Chaïeb, E., Bouyanzer, A., Hammouti, B., Benkaddour, M., Berrabah, M., 2004. *Trans. SAEST* 39, 58.
- Chaïeb, E., Bouyanzer, A., Hammouti, B., Benkaddour, M., 2005. *Appl. Surf. Sci.* 246, 199.
- Chaïeb, E., Bouyanzer, A., Hammouti, B., Berrabah, M., 2009. *Acta Phys. Chim. Sin.* 25, 1254.
- Chauhan, L.R., Gunasekaran, G., 2007. *Corros. Sci.* 49, 1143.
- Chetouani, A., Hammouti, B., Benkaddour, M., 2004. *Pigm. Resin Technol.* 33, 26.
- Clevenger, J.F., 1928. *J. Am. Pharm. Assoc.* 17, 346.
- de Boer, J.H., 1968. *The Dynamical Character of Adsorption*, second ed. Clarendon Press, Oxford, UK.
- Eddy, N.O., Ebenso, E.E., 2008. *Afr. J. Pure Appl. Chem.* 2, 46.
- Eddy, N.O., Odoemelam, S.A., 2008. *Mater. Sci. (India)* 4, 9.
- El-Ashry, E.H., El-Nemir, A., Esawy, S.A., Ragab, S., 2006. *Electrochim. Acta* 51, 3957.
- El-Ouariachi, E., Paolini, J., Bouklah, M., Elidrissi, A., Bouyanzer, A., Hammouti, B., Desjobert, J.-M., Costa, J., 2010. *Acta Metall. Sin.* 23, 13.
- Faska, Z., Majidi, L., Fihî, R., Bouyanzer, A., Hammouti, B., 2007. *Pigm. Resin Technol.* 36, 293.
- Faska, Z., Bellioua, A., Bouklah, M., Majidi, L., Fihî, R., Bouyanzer, A., Hammouti, B., 2008. *Monatsh. Chem.* 139, 1417.
- Frumkin, A.N.Z., 1925. *Phys. Chem.* 116, 466.
- Holemen, M., Berradi, M., Bellakhder, J., Idrissi, A., Pinel, R., 1984. *Fitoterapia* 55, 143.
- Ipek, A., Gürbüz, B., Sarihan, E.O., Duran, A., Kendir, H., 2008. *J. Appl. Biol. Sci.* 2, 99.
- Juttner, K., 1990. *Electrochim. Acta* 35, 1501.
- König, W.A., Hochmuth, D.H., Joulain, D., 2001. *Terpenoids and Related Constituents of Essential Oils. Library of MassFinder 2.1.* Institute of Organic Chemistry, Hamburg, Germany.
- Kürkcüoğlu, M., Baser, K.H., Essent, J., 2002. *Oil Res.* 14, 241.
- Langmuir, I., 1947. *J. Am. Chem. Soc.* 39, 1848.
- Larabi, L., Harek, Y., Traisnel, M., Mansri, A., 2004. *J. Appl. Electrochem.* 34, 833.
- Mansfeld, F., Kending, M.W., Tsai, S., 1981. *Corrosion* 37, 301.
- Mansfeld, F., Kending, M.W., Tsai, S., 1982. *Corrosion* 38, 570.
- Martinez, S., Metikos-Hukovic, M., 2003. *J. Appl. Electrochem.* 33, 1137.
- Masel, R.I., 1996. *Principles of Adsorption and Reaction on Solid Surfaces.* Willey, New York.
- Ouachikh, O., Bouyanzer, A., Bouklah, M., Desjobert, J.-M., Costa, J., Hammouti, B., Majidi, L., 2009. *Surf. Rev. Lett.* 16, 49.
- Ozcan, M., 2005. *J. Med. Food* 8, 110.
- Pajkosay, T., 1994. *J. Electroanal. Chem.* 364, 111.
- Popova, A., Christov, M., Raicheva, S., Sokolova, E., 2004. *Corros. Sci.* 46, 1333.
- Sethuran, M.G., Raja, P.B., 2006. *Pigm. Resin Technol.* 34, 327.
- Tsuru, T., Haruyama, S., Gijutsu, B., 1978. *J. Jpn. Soc. Corros. Eng.* 27, 573.
- Zerga, B., Sfaira, M., Rais, Z., Ebn Touhami, M., Taleb, M., Hammouti, B., Imelouane, B., Elbachiri, A., 2009. *Mater. Technol.* 97, 297.